

Computational Science Laboratory Technical Report

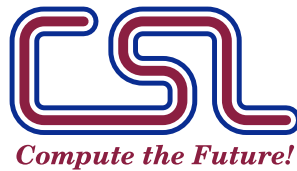
CSL-TR-19-1

June 28, 2022

Arash Sarshar and Adrian Sandu

*“Alternating Directions Implicit
Integration in a General Linear
Method Framework”*

Computer Science Department
Virginia Polytechnic Institute and State University
Blacksburg, VA 24060
Phone: (540)-231-2193
Fax: (540)-231-6075
Email: sarshar@vt.edu
Web: <http://csl.cs.vt.edu>



Alternating Directions Implicit Integration in a General Linear Method Framework

Arash Sarshar^{a,*}, Adrian Sandu^a

^a*Computational Science Laboratory
Department of Computer Science
Virginia Tech*

Abstract

Alternating Directions Implicit (ADI) integration is an operator splitting approach to solve parabolic and elliptic partial differential equations in multiple dimensions based on solving sequentially a set of related one-dimensional equations. Classical ADI methods have order at most two, due to the splitting errors. Moreover, when the time discretization of stiff one-dimensional problems is based on Runge-Kutta schemes, additional order reduction may occur. This work proposes a new ADI approach based on the partitioned General Linear Methods framework. This approach allows the construction of high order ADI methods. Due to their high stage order, the proposed methods can alleviate the order reduction phenomenon seen with other schemes. Numerical experiments are shown to provide further insight into the accuracy, stability and applicability of these new methods.

Keywords: Initial value problems, time integration, IMEX methods, alternating directions AMS 65L05, AMS 65L07

1. Introduction

We are concerned with solving the initial value problem:

$$y'(t) = f(y) = \sum_{\sigma=1}^N f^{\{\sigma\}}(y), \quad y(t_0) = y_0, \quad (1)$$

*Corresponding author

Email addresses: sarshar@vt.edu (Arash Sarshar), sandu@cs.vt.edu (Adrian Sandu)

where the right hand side function $f : \mathbb{R}^d \rightarrow \mathbb{R}^d$ is additively split into N partitions. Systems such as eq. (1) emerge from method of lines semi-discretization of PDEs when all spatial derivatives are approximated by their discretization. In 5 many cases, the right hand side function includes discrete self-adjoint operators performing spatial derivatives in different directions. The sparsity structure of these operators is similar, for example, in the case when a fixed-stencil finite difference method is used to resolve spatial derivatives. Implicit time-stepping methods are preferred to propagate stiff differential equations in time, but they 10 require working with large Jacobian matrices. IMEX methods allow us to integrate non-stiff parts of the system more efficiently, however, more can be achieved by designing specialized time-stepping methods for certain classes of problems. Depending on the choice of discretization, we can leverage the tensor 15 product structure of derivative operators to only work with one-dimensional Jacobian matrices much smaller than the full Jacobian, applying directional derivatives in different directions in turn. This paper is concerned with developing high order GLM methods suited for alternating directions implicit integration.

Early analysis of convergence for stiff ODEs can be traced back to Prothero-Robinson [1]. Ostermann *et al.* formally show the fractional order phenomenon 20 is related to changes in local truncation error behavior in stiff systems [2]. Methods of high stage order are known to alleviate this drawback. The General Linear Methods (GLM) framework [3–5] encompasses many of these methods and facilitates creation of new ones for novel applications. The theory of partitioned 25 GLMs was developed in [6]. Based on this theory, high order implicit-explicit (IMEX) GLMs were developed in [7–10], and provide an important foundation for the goals of this paper.

Although ADI schemes have been around for decades [11], we are particularly 30 inspired by the work [12–14] on Approximate Matrix Factorizations (AMF) applied to Implicit Runge-Kutta and Rosenbrock-type methods leading to high order ADI methods suitable for a range of stiff problems including Advection-Reaction-Diffusion and mixed-derivative parabolic PDEs[15].

The paper is organized as follows. We start by reviewing the partitioned

GLM framework in section 2, introduce the structure of ADI GLM methods in section 3, study their order conditions in section 4, and investigate their stability in section 5. We briefly comment on design principles and implementation aspects in section 6 followed by numerical experiments in section 7 and the concluding remarks in section 8. Appendix A includes the coefficients of the new methods, and Appendix B presents stability plots.

2. Traditional and partitioned General Linear Methods

A traditional GLM with s internal and r external stages represented by Butcher tableau:

$$\begin{array}{c|cc|c} \mathbf{c} & \mathbf{A} & \mathbf{U} \\ \hline & \mathbf{B} & \mathbf{V} \end{array}, \quad (2)$$

advances the numerical solution to eq. (1) with timestep h according to:

$$Y_i = h \sum_{j=1}^s a_{i,j} f(Y_j) + \sum_{j=1}^r u_{i,j} \xi_j^{[n-1]}, \quad i = 1, \dots, s, \quad (3a)$$

$$\xi_i^{[n]} = h \sum_{j=1}^s b_{i,j} f(Y_j) + \sum_{j=1}^r v_{i,j} \xi_j^{[n-1]}, \quad i = 1, \dots, r, \quad (3b)$$

where the matrix notation of coefficients is used:

$$\begin{aligned} \mathbf{A} &:= [a_{i,j}] \in \mathbb{R}^{s \times s}, & \mathbf{U} &:= [u_{i,j}] \in \mathbb{R}^{s \times r}, & \mathbf{B} &:= [b_{i,j}] \in \mathbb{R}^{r \times s}, \\ \mathbf{V} &:= [v_{i,j}] \in \mathbb{R}^{r \times r}, & \mathbf{W} &:= [w_{i,j}] = [\mathbf{w}_0 \cdots \mathbf{w}_p] \in \mathbb{R}^{(p+1) \times r}. \end{aligned} \quad (4)$$

GLM framework is extensive and well-established. Readers interested in theoretical foundation of these methods are referred to the literature [3–5].

IMEX-GLMs are extensions of traditional GLMs that treat partitions of the right hand with different methods while keeping a single set of internal and external stages. One step of an IMEX-GLM formally reads as:

$$Y_i = h \sum_{\sigma=1}^N \sum_{j=1}^s a_{i,j}^{\{\sigma\}} f^{\{\sigma\}}(Y_j) + \sum_{j=1}^r u_{i,j} \xi_j^{[n-1]}, \quad i = 1, \dots, s, \quad (5a)$$

$$\xi_i^{[n]} = h \sum_{\sigma=1}^N \sum_{j=1}^s b_{i,j}^{\{\sigma\}} f^{\{\sigma\}}(Y_j) + \sum_{j=1}^r v_{i,j} \xi_j^{[n-1]}, \quad i = 1, \dots, r. \quad (5b)$$

3. Formulation of ADI-GLMs

We rely on the theory of IMEX-GLMs as reported in [6–10] to design partitioned GLMs suited for ADI integration. The goal is to construct GLMs that apply implicit integration to individual partitions of the right hand side function in eq. (1), while using an explicit coupling to the other components. We seek to achieve high stage order while benefiting from the low computational cost of directional implicit methods.

Definition 1 (ADI-GLM schemes). *One step of an N -way partitioned ADI-GLM applied to eq. (1) is defined as:*

$$Y_i^{\{\mu\}} = h \sum_{\sigma=1}^N \sum_{j=1}^s a_{i,j}^{\{\mu,\sigma\}} f^{\{\sigma\}}(Y_j^{\{\sigma\}}) + \sum_{\sigma=1}^N \sum_{j=1}^r u_{i,j}^{\{\mu,\sigma\}} \xi_j^{\{\sigma\}[n-1]}, \quad (6a)$$

$$i = 1, \dots, s, \quad \mu = 1, \dots, N,$$

$$\xi_i^{\{\mu\}[n]} = h \sum_{\sigma=1}^N \sum_{j=1}^s b_{i,j}^{\{\mu,\sigma\}} f^{\{\sigma\}}(Y_j^{\{\sigma\}}) + \sum_{\sigma=1}^N \sum_{j=1}^r v_{i,j}^{\{\mu,\sigma\}} \xi_j^{\{\sigma\}[n-1]}, \quad (6b)$$

$$i = 1, \dots, r.$$

Here, we are interested in applying different combinations of explicit and diagonally implicit methods to the right hand side partitions and storing the resulting internal stages separately. As a consequence, we may have to carry separate external stages, but this comes at no extra cost as they are linear combinations of previously computed values.

If the method is order p , the external stages are related to derivatives of y by:

$$\xi_i^{\{\mu\}[n]} = w_{i,0}^{\{\mu\}} y(t_n) + \sum_{\sigma=1}^N \sum_{k=1}^p w_{i,k}^{\{\mu,\sigma\}} h^k (f^{\{\sigma\}})^{(k-1)}(y_n) + \mathcal{O}(h^{p+1}), \quad (7)$$

$$\mathbf{W}^{\{\mu,\sigma\}} := [\mathbf{w}_0^{\{\mu\}} \ \dots \ \mathbf{w}_p^{\{\mu,\sigma\}}] \in \mathbb{R}^{(p+1) \times r}. \quad (8)$$

The method is stage order q if internal stages are approximations of the exact solution at abscissa points $\mathbf{c}^{\{\mu\}}$:

$$Y_i^{\{\mu\}} = y(t_{n-1} + \mathbf{c}_i^{\{\mu\}} h) + \mathcal{O}(h^{q+1}). \quad (9)$$

4. Construction of ADI-GLMs

We start by considering a pair of explicit and implicit GLMs with the same number of external and internal stages:

$$\frac{\mathbf{c}^{\{E\}} \mid \mathbf{A}^{\{E\}} \mid \mathbf{U}^{\{E\}}}{\mathbf{B}^{\{E\}} \mid \mathbf{V}^{\{E\}}}, \quad \frac{\mathbf{c}^{\{I\}} \mid \mathbf{A}^{\{I\}} \mid \mathbf{U}^{\{I\}}}{\mathbf{B}^{\{I\}} \mid \mathbf{V}^{\{I\}}}. \quad (10)$$

The order conditions for the two methods are as follows [16]:

$$\frac{\mathbf{c}^{\{\sigma\} \times k}}{k!} - \frac{\mathbf{A} \mathbf{c}^{\{\sigma\} \times (k-1)}}{(k-1)!} - \mathbf{U}^{\{\sigma\}} \mathbf{w}_k^{\{\sigma\}} = 0, \quad (11a)$$

$$k = \{1, \dots, q\}, \quad \sigma \in \{E, I\},$$

$$\sum_{l=0}^k \frac{\mathbf{w}_{k-l}^{\{\sigma\}}}{l!} - \frac{\mathbf{B}^{\{\sigma\}} \mathbf{c}^{\{\sigma\} \times (k-1)}}{(k-1)!} - \mathbf{V}^{\{\sigma\}} \mathbf{w}_k^{\{\sigma\}} = 0, \quad (11b)$$

$$k = \{1, \dots, p\}, \quad \sigma \in \{E, I\}.$$

55

We construct ADI-GLM methods using a collection of IMEX-GLM methods each performing implicit integration in a specific direction. The structure of the Butcher tableau for an ADI-GLM depends on the number of partitions and number of stiff partitions that require implicit treatment. Here, we focus on three practical examples and more elaborate designs follow the same principles. The Butcher tableau for a 3-way partitioned ADI-GLM method with alternating implicit stages in all partitions is:

$$\begin{array}{c|ccc|ccc} \mathbf{c} & \mathbf{A}^{\{I\}} & \mathbf{A}^{\{E\}} & \mathbf{A}^{\{E\}} & \mathbf{U} & \mathbf{0} & \mathbf{0} \\ \mathbf{c} & \mathbf{A}^{\{I\}} & \mathbf{A}^{\{I\}} & \mathbf{A}^{\{E\}} & \mathbf{0} & \mathbf{U} & \mathbf{0} \\ \mathbf{c} & \mathbf{A}^{\{I\}} & \mathbf{A}^{\{I\}} & \mathbf{A}^{\{I\}} & \mathbf{0} & \mathbf{0} & \mathbf{U} \\ \hline & \mathbf{B}^{\{I\}} & \mathbf{B}^{\{E\}} & \mathbf{B}^{\{E\}} & \mathbf{V} & \mathbf{0} & \mathbf{0} \\ & \mathbf{B}^{\{I\}} & \mathbf{B}^{\{I\}} & \mathbf{B}^{\{E\}} & \mathbf{0} & \mathbf{V} & \mathbf{0} \\ & \mathbf{B}^{\{I\}} & \mathbf{B}^{\{I\}} & \mathbf{B}^{\{I\}} & \mathbf{0} & \mathbf{0} & \mathbf{V} \end{array}. \quad (12)$$

When only two partitions are stiff, the non-stiff partition is carried through

explicitly:

$$\begin{array}{c|ccc|ccc} \mathbf{c} & \mathbf{A}^{\{I\}} & \mathbf{A}^{\{E\}} & \mathbf{A}^{\{E\}} & \mathbf{U} & \mathbf{0} & 0 \\ \mathbf{c} & \mathbf{A}^{\{I\}} & \mathbf{A}^{\{I\}} & \mathbf{A}^{\{E\}} & \mathbf{0} & \mathbf{U} & 0 \\ \mathbf{c} & \mathbf{A}^{\{I\}} & \mathbf{A}^{\{I\}} & \mathbf{A}^{\{E\}} & \mathbf{0} & 0 & \mathbf{U} \\ \hline & \mathbf{B}^{\{I\}} & \mathbf{B}^{\{E\}} & \mathbf{B}^{\{E\}} & \mathbf{V} & \mathbf{0} & 0 \\ & \mathbf{B}^{\{I\}} & \mathbf{B}^{\{I\}} & \mathbf{B}^{\{E\}} & \mathbf{0} & \mathbf{V} & 0 \\ & \mathbf{B}^{\{I\}} & \mathbf{B}^{\{I\}} & \mathbf{B}^{\{E\}} & \mathbf{0} & 0 & \mathbf{V} \end{array}. \quad (13)$$

We notice immediately that $Y_i^{\{3\}} \equiv Y_i^{\{2\}}$, therefore one only computes two types of stage vectors, and the second is used as an argument for the explicit integration of the third, non-stiff component.

In a similar fashion, a 2-way partitioned ADI-GLM is described by:

$$\begin{array}{c|cc|cc} \mathbf{c} & \mathbf{A}^{\{I\}} & \mathbf{A}^{\{E\}} & \mathbf{U} & \mathbf{0} \\ \mathbf{c} & \mathbf{A}^{\{I\}} & \mathbf{A}^{\{I\}} & \mathbf{0} & \mathbf{U} \\ \hline & \mathbf{B}^{\{I\}} & \mathbf{B}^{\{E\}} & \mathbf{V} & \mathbf{0} \\ & \mathbf{B}^{\{I\}} & \mathbf{B}^{\{I\}} & \mathbf{0} & \mathbf{V} \end{array}. \quad (14)$$

Remark 1. Comparing eqs. (12) to (14) with eq. (6), notice that we have chosen:

$$\mathbf{c}^{\{E\}} = \mathbf{c}^{\{I\}} = \mathbf{c}, \quad (15a)$$

$$\mathbf{U}^{\{E\}} = \mathbf{U}^{\{I\}} = \mathbf{U}, \quad (15b)$$

$$\mathbf{V}^{\{E\}} = \mathbf{V}^{\{I\}} = \mathbf{V}. \quad (15c)$$

This selection is practically useful in creating IMEX-GLM methods with unified internal stages. In the context of ADI-GLMs this choice allows us to keep the number of internal and external stages as low as the number of stiff partitions.

Remark 2. We have also decoupled computations involving the external stages:

$$\mathbf{U}^{\{\sigma, \mu\}} = \begin{cases} \mathbf{0} & \sigma \neq \mu \\ \mathbf{U} & \sigma = \mu \end{cases}, \quad \mathbf{V}^{\{\sigma, \mu\}} = \begin{cases} \mathbf{0} & \sigma \neq \mu \\ \mathbf{V} & \sigma = \mu \end{cases}. \quad (16)$$

Theorem 1. *The ADI-GLM method eq. (6) subject to eqs. (15) and (16) is stage order q and order p , hereafter denoted by order (q, p) , if and only if individual methods (10) are order (q, p) .*

Proof. We first assume that the ADI-GLM is order (q, p) such that eqs. (7) and (9) hold. Since all internal stages $Y_i^{\{\sigma\}}$ share the same abscissa, from eq. (9) we have:

$$Y_i^{\{\sigma\}} = Y_i^{\{\mu\}} + \mathcal{O}(h^{q+1}), \quad \sigma, \mu \in \{1, \dots, N\}. \quad (17)$$

Therefore, we can replace $Y_j^{\{\sigma\}}$ with $Y_j^{\{\mu\}}$ in eq. (6a) without changing the order. The resulting method is an IMEX-GLM with

$$\begin{array}{c|ccccc|c} \mathbf{c} & \mathbf{A}^{\{\mu,1\}} & \dots & \mathbf{A}^{\{\mu,N\}} & & & \mathbf{U} \\ \hline & \mathbf{B}^{\{\mu,1\}} & \dots & \mathbf{B}^{\{\mu,N\}} & & & \mathbf{V} \end{array}, \quad \mu \in \{1, \dots, N\}. \quad (18)$$

From IMEX-GLM order conditions [6, 16] method (18) is order (q, p) if and only if individual methods

$$\begin{array}{c|ccccc|c} \mathbf{c} & \mathbf{A}^{\{\mu,\sigma\}} & & & & & \mathbf{U} \\ \hline & \mathbf{B}^{\{\mu,\sigma\}} & & & & & \mathbf{V} \end{array}, \quad \mu \in \{1, \dots, N\}, \quad \sigma \in \{1, \dots, N\}.$$

are order (q, p) . This means that the methods in (10) have to be order (q, p) .

The *if* part of the theorem can be proven along the same line of reasoning. Assuming individual methods (10) are order (q, p) the IMEX-GLM method (18) is order (q, p) . Internal stage values in eq. (5a) can be replaced by an approximation of the same order as in eq. (17) to create the internal stages for ADI-GLM method. Since the order of internal stages has not changed, external stages also remain order p . This concludes the proof. \square

Remark 3. *A corollary to theorem 1 is that in the case of ADI-GLM (13), we can forgo computing $(Y_i^{\{3\}}, \xi^{\{3\}[n]})$ stages without losing accuracy. Furthermore, this choice will not affect the stability since the stiff partitions are still treated implicitly and the integration of the non-stiff partition already appears in stage computations.*

5. Stability of ADI-GLMs

Applying the ADI-GLM (12) to the linear scalar test equation:

$$u' = \lambda_x u + \lambda_y u + \lambda_z u, \quad (19)$$

and using eq. (6) leads to the following directional stages:

$$Y^{\{1\}} = \eta_x \mathbf{A}^{\{I\}} Y^{\{1\}} + \eta_y \mathbf{A}^{\{E\}} Y^{\{2\}} + \eta_z \mathbf{A}^{\{E\}} Y^{\{3\}} + \mathbf{U} \xi^{\{1\}[n-1]}, \quad (20a)$$

$$Y^{\{2\}} = \eta_x \mathbf{A}^{\{I\}} Y^{\{1\}} + \eta_y \mathbf{A}^{\{I\}} Y^{\{2\}} + \eta_z \mathbf{A}^{\{E\}} Y^{\{3\}} + \mathbf{U} \xi^{\{2\}[n-1]}, \quad (20b)$$

$$Y^{\{3\}} = \eta_x \mathbf{A}^{\{I\}} Y^{\{1\}} + \eta_y \mathbf{A}^{\{I\}} Y^{\{2\}} + \eta_z \mathbf{A}^{\{I\}} Y^{\{3\}} + \mathbf{U} \xi^{\{3\}[n-1]}, \quad (20c)$$

$$\xi^{\{1\}[n]} = \eta_x \mathbf{B}^{\{I\}} Y^{\{1\}} + \eta_y \mathbf{B}^{\{E\}} Y^{\{2\}} + \eta_z \mathbf{B}^{\{E\}} Y^{\{3\}} + \mathbf{V} \xi^{\{1\}[n-1]}, \quad (20d)$$

$$\xi^{\{2\}[n]} = \eta_x \mathbf{B}^{\{I\}} Y^{\{1\}} + \eta_y \mathbf{B}^{\{E\}} Y^{\{2\}} + \eta_z \mathbf{B}^{\{E\}} Y^{\{3\}} + \mathbf{V} \xi^{\{2\}[n-1]}, \quad (20e)$$

$$\xi^{\{3\}[n]} = \eta_x \mathbf{B}^{\{I\}} Y^{\{1\}} + \eta_y \mathbf{B}^{\{I\}} Y^{\{2\}} + \eta_z \mathbf{B}^{\{I\}} Y^{\{3\}} + \mathbf{V} \xi^{\{3\}[n-1]}, \quad (20f)$$

where $\eta_x = h\lambda_x$, $\eta_y = h\lambda_y$, $\eta_z = h\lambda_z$. The stability matrix is defined as:

$$\xi^{[n]} = \mathbf{M}(\eta) \xi^{[n-1]}, \quad \xi^{[n]} = \left(\xi^{\{1\}[n]}, \xi^{\{2\}[n]}, \xi^{\{3\}[n]} \right)^T, \quad (21a)$$

$$\eta = (\eta_x, \eta_y, \eta_z)^T, \quad \mathbf{J} = \text{diag}(\eta) \otimes \mathbf{I}_{s \times s},$$

$$\mathbf{M}(\eta) = \tilde{\mathbf{V}} + \tilde{\mathbf{B}} \mathbf{J} \left(\mathbf{I}_{3s \times 3s} - \tilde{\mathbf{A}} \mathbf{J} \right)^{-1} \tilde{\mathbf{U}}, \quad (21b)$$

where \otimes represents the Kronecker product and:

$$\tilde{\mathbf{A}} = \begin{pmatrix} \mathbf{A}^{\{I\}} & \mathbf{A}^{\{E\}} & \mathbf{A}^{\{E\}} \\ \mathbf{A}^{\{I\}} & \mathbf{A}^{\{I\}} & \mathbf{A}^{\{E\}} \\ \mathbf{A}^{\{I\}} & \mathbf{A}^{\{I\}} & \mathbf{A}^{\{I\}} \end{pmatrix}, \quad \tilde{\mathbf{U}} = \mathbf{I}_{3 \times 3} \otimes \mathbf{U}, \quad (22a)$$

$$\tilde{\mathbf{B}} = \begin{pmatrix} \mathbf{B}^{\{I\}} & \mathbf{B}^{\{E\}} & \mathbf{B}^{\{E\}} \\ \mathbf{B}^{\{I\}} & \mathbf{B}^{\{I\}} & \mathbf{B}^{\{E\}} \\ \mathbf{B}^{\{I\}} & \mathbf{B}^{\{I\}} & \mathbf{B}^{\{I\}} \end{pmatrix}, \quad \tilde{\mathbf{V}} = \mathbf{I}_{3 \times 3} \otimes \mathbf{V}. \quad (22b)$$

Two special cases are noteworthy. First, when the eigenvalues of the system (19) are equal in all directions such that $\eta_x = \eta_y = \eta_z = \eta$ the stability matrix becomes:

$$\widehat{\mathbf{M}}(\eta) = \tilde{\mathbf{V}} + \eta \tilde{\mathbf{B}} \left(\mathbf{I}_{3s \times 3s} - \eta \tilde{\mathbf{A}} \right)^{-1} \tilde{\mathbf{U}}. \quad (23)$$

The second marginal case is when the system becomes infinitely stiff:

$$\mathbf{M}_\infty = \lim_{\eta \rightarrow -\infty} \widehat{\mathbf{M}}(\eta) = \tilde{\mathbf{V}} - \tilde{\mathbf{B}} \tilde{\mathbf{A}}^{-1} \tilde{\mathbf{U}}. \quad (24)$$

Equations (23) and (24) provide practical means for assessment and optimization of stability of ADI-GLM methods.

Remark 4. *The stability regions for individual explicit and implicit methods are defined as:*

$$\mathcal{S}^{\{\sigma\}} = \left\{ \eta \in \mathbb{C}^- : \rho(\mathbf{M}^{\{\sigma\}}(\eta)) < 1 \right\}, \quad (25a)$$

$$\mathbf{M}^{\{\sigma\}}(\eta) = \mathbf{V}^{\{\sigma\}} + \eta \mathbf{B}^{\{\sigma\}} \left(\mathbf{I}_{s \times s} - \eta \mathbf{A}^{\{\sigma\}} \right)^{-1} \mathbf{U}^{\{\sigma\}}, \quad \sigma \in \{E, I\}, \quad (25b)$$

where $\rho(\cdot)$ denotes the spectral radius operator. The stability region a 3-way partition method is defined as:

$$S = \left\{ \eta \in \mathbb{C}^- \times \mathbb{C}^- \times \mathbb{C}^- : \rho(\mathbf{M}(\eta)) < 1 \right\}. \quad (26)$$

Remark 5. *To investigate the stability of ADI-DIMSIM methods we define real and complex stability regions as:*

$$\mathcal{S}_{\text{Real}} = \left\{ \eta \in \mathbb{R}^- \times \mathbb{R}^- : \rho(\mathbf{M}(\eta_x, \eta_y, \max(\eta_x, \eta_y))) < 1 \right\}, \quad (27a)$$

$$\mathcal{S}_{\text{Cplx}} = \left\{ \eta \in \mathbb{C}^- : \rho(\widehat{\mathbf{M}}(\eta)) < 1 \right\}. \quad (27b)$$

80 In Appendix B we provide plots of different stability regions for ADI-GLM methods.

6. Design and implementation of ADI-GLMs

We have chosen the GLM methods to be DIMSIMs [17] in order to reduce the number of free parameters in the design and simplify the order conditions. We require:

$$a_{i,i}^{\{I\}} = \gamma, \quad a_{i,i}^{\{E\}} = 0, \quad a_{i,j}^{\{\sigma\}} = 0, \quad \text{for } j > i, \quad \sigma \in \{E, I\}, \quad (28a)$$

$$\mathbf{U}^{\{\sigma\}} = \mathbf{I}_{s \times r}, \quad \sigma \in \{E, I\}, \quad (28b)$$

$$\mathbf{V}^{\{\sigma\}} = \mathbb{1}^T v^{\{\sigma\}}, \quad v^{\{\sigma\}T} \mathbb{1} = 1, \quad \sigma \in \{E, I\}, \quad (28c)$$

where $v^{\{\sigma\}}, \mathbf{1} \in \mathbb{R}^s$ and $\mathbf{1}$ is the unit vector in that space. ADI–DIMSIM methods derived in this paper have $p = q = r = s$. The design process starts with choosing the abscissa vector \mathbf{c} . The remaining free parameters are coefficients of $\mathbf{A}^{\{E\}}$, $\mathbf{A}^{\{I\}}$ and v . $\mathbf{A}^{\{E\}}$ is chosen such that $\mathcal{S}^{\{E\}}$ is sufficiently large. $\mathbf{A}^{\{I\}}$ and v are used to optimize stability of ADI–DIMSIM methods. To further narrow down the parameter space, the following stability criteria may be considered in the form of algebraic root equations:

$$\lim_{z \rightarrow -\infty} \rho(\mathbf{M}^{\{I\}}(z)) = 0, \quad (29)$$

$$\mathbf{M}_\infty \text{ is power bounded.} \quad (30)$$

For methods of order 2 and 3 these conditions can be conveniently calculated in Mathematica along with analytical expressions for the eigenvalues of $\widehat{\mathbf{M}}(z)$ to derive method coefficients. The ADI–DIMSIM4 method is derived by solving a numerical optimization in Matlab that maximizes the stability region $\mathcal{S}_{\text{Real}}$ through sampling. The results of numerical optimization is then imported back into Mathematica and used to solve for a nearby infinite-precision solution.

Once $\mathbf{A}^{\{E\}}$ and $\mathbf{A}^{\{I\}}$ and \mathbf{V} are determined, $\mathbf{B}^{\{E\}}$ and $\mathbf{B}^{\{I\}}$ are given using DIMSIM formulas [18, 19]. $\mathbf{W}^{\{I\}}$ and $\mathbf{W}^{\{E\}}$ are computed by solving eq. (11) and used in the starting procedure to generate initial values of the external stages at the beginning of the time-stepping loop in eq. (6). The starting procedure consists of integrating the system eq. (1) exactly over a short time-span $[0, pH]$ and using function values

$$f_k^{\{\sigma\}} := f^{\{\sigma\}}(y(kH)), \quad k = \{0, \dots, p\}, \quad \sigma \in \{1, \dots, N\}, \quad (31)$$

to approximate, via divided differences, the higher order derivatives needed in eq. (7). Readers interested in further details about the starting procedure may consult [6, 20]. The ending procedure for GLM methods produces the high order approximation to $y(t_f)$ at the final time using stage values. All ADI–GLM methods designed in this paper have the property that $\mathbf{c}_s = 1$, therefore, the last computed internal stage may be used as the final value in the integration

with no further calculation required:

$$y_{tf} = Y_s^{\{\mathcal{N}_s\}} = h \sum_{\sigma=1}^N \sum_{j=1}^s a_{s,j}^{\{\mathcal{N}_s, \sigma\}} f^{\{\sigma\}}(Y_j^{\{\sigma\}}) + \sum_{j=1}^r u_{s,j}^{\{\mathcal{N}_s, \sigma\}} \xi_j^{\{\sigma\}[n-1]}. \quad (32)$$

Remark 6 (The ADI character of the methods). *The Butcher tableau for ADI-DIMSIMs can be permuted to reflect the order of computation of stages in practice. In general, an ADI-GLM proceeds with computing internal stages:*

$$\left\{ Y_1^{\{1\}}, Y_1^{\{2\}}, \dots, Y_1^{\{N\}}, \dots, Y_s^{\{1\}}, \dots, Y_s^{\{2\}}, \dots, Y_s^{\{N\}} \right\}, \quad (33)$$

after which external stage updates are computed. Let us consider application of ADI-DIMSIM2 method in Appendix A.1 to (14) where we have tabulated the coefficients in 34. We reorder the tableau according to the permutation list $\mathcal{P} = \{1, 3, 2, 4\}$ to get the permuted tableau (35).

$$\begin{array}{c|c|c|c|c|c} \mathbf{c} & \mathbf{A} & \mathbf{U} & & & \\ \hline & 0 & \frac{5}{8} & 0 & 0 & 0 \\ & 1 & \frac{1}{4} & \frac{5}{8} & \frac{1}{2} & 0 \\ & 0 & \frac{5}{8} & 0 & \frac{5}{8} & 0 \\ \hline & 1 & \frac{1}{4} & \frac{5}{8} & \frac{1}{4} & \frac{5}{8} \\ \hline \mathbf{B} & \mathbf{V} & & & & \\ \hline & \frac{1}{2} & -\frac{5}{32} & -\frac{3}{128} & \frac{5}{128} & -\frac{5}{16} \frac{21}{16} 0 0 \\ & 0 & \frac{27}{32} & \frac{13}{128} & \frac{85}{128} & -\frac{5}{16} \frac{21}{16} 0 0 \\ & -\frac{3}{128} & \frac{5}{128} & -\frac{3}{128} & \frac{5}{128} & 0 0 -\frac{5}{16} \frac{21}{16} \\ & \frac{13}{128} & \frac{85}{128} & \frac{13}{128} & \frac{85}{128} & 0 0 -\frac{5}{16} \frac{21}{16} \end{array}, \quad (34)$$

$$\begin{array}{c|c|c|c|c|c} \mathbf{c} & \mathbf{A}_{\mathcal{P}, \mathcal{P}} & \mathbf{U}_{\mathcal{P}, :} & & & \\ \hline & 0 & \frac{5}{8} & 0 & 0 & 0 \\ & 0 & \frac{5}{8} & 0 & 0 & 0 \\ & 1 & \frac{1}{4} & \frac{1}{2} & \frac{5}{8} & 0 \\ \hline & 1 & \frac{1}{4} & \frac{1}{4} & \frac{5}{8} & \frac{5}{8} \\ \hline \mathbf{B}_{:, \mathcal{P}} & \mathbf{V} & & & & \\ \hline & \frac{1}{2} & -\frac{3}{128} & -\frac{5}{32} & \frac{5}{128} & -\frac{5}{16} \frac{21}{16} 0 0 \\ & 0 & \frac{13}{128} & \frac{27}{32} & \frac{85}{128} & -\frac{5}{16} \frac{21}{16} 0 0 \\ & -\frac{3}{128} & -\frac{3}{128} & \frac{5}{128} & \frac{5}{128} & 0 0 -\frac{5}{16} \frac{21}{16} \\ & \frac{13}{128} & \frac{13}{128} & \frac{85}{128} & \frac{85}{128} & 0 0 -\frac{5}{16} \frac{21}{16} \end{array}. \quad (35)$$

We observe how the lower triangular structure of $\mathbf{A}_{\mathcal{P}, \mathcal{P}}$ defines successive implicit stages in different directions, while using previously computed stage values explicitly.

7. Numerical Experiments

In this section we investigate numerically the accuracy and stability of ADI–DIMSIM methods using 2D and 3D parabolic PDEs. For a 3D problem we use the equation:

$$\frac{\partial u}{\partial t} = \frac{\partial^2 u}{\partial x^2} + \frac{\partial^2 u}{\partial y^2} + \frac{\partial^2 u}{\partial z^2} + g(x, y, z, t), \quad (36a)$$

$$\begin{aligned} g(x, y, z, t) = & e^t(1-x)x(1-y)y(1-z)z \\ & + 2e^t(1-x)x(1-y)y + 2e^t(1-x)x(1-z)z \\ & + 2e^t(1-y)y(1-z)z - 6e^t \\ & + e^t \left(\left(x + \frac{1}{3} \right)^2 + \left(y + \frac{1}{4} \right)^2 + \left(z + \frac{1}{2} \right)^2 \right), \end{aligned} \quad (36b)$$

with Dirichlet boundary conditions according to the exact solution:

$$u(x, y, z, t) = e^t(1-x)x(1-y)y(1-z)z \quad (37)$$

$$+ e^t \left(\left(x + \frac{1}{3} \right)^2 + \left(y + \frac{1}{4} \right)^2 + \left(z + \frac{1}{2} \right)^2 \right). \quad (38)$$

The spatial discretization uses second order finite differences on the unit cube domain $D := \{x, y, z \in [0, 1]\}$ with a uniform mesh with N_p points in each direction. We use the parameter N_p in our experiments to vary the stiffness of directional derivatives. Note that using a uniform mesh allows us to factorize a tri-diagonal one-dimensional Jacobian matrix once and use it to efficiently to compute directional stages.

To verify the temporal order of convergence for the new methods we integrate the problem over a time-span $t = [0, 1]$ and record the normalized L_2 error at final time versus number of time steps. Figures 1a to 1c, verifies the theoretical order for a range of mesh sizes. We compare ADI–DIMSIM methods with an ADI scheme based on a fourth order IMEX Runge–Kutta method reported in [21]. We note the deterioration in the order as the problem becomes more stiff with decreasing mesh size in fig. 1d.

For a 2D numerical experiment the following problem is used on unit square domain $D = \{x, y \in [0, 1]\}$, with the same spatial discretization and integrated

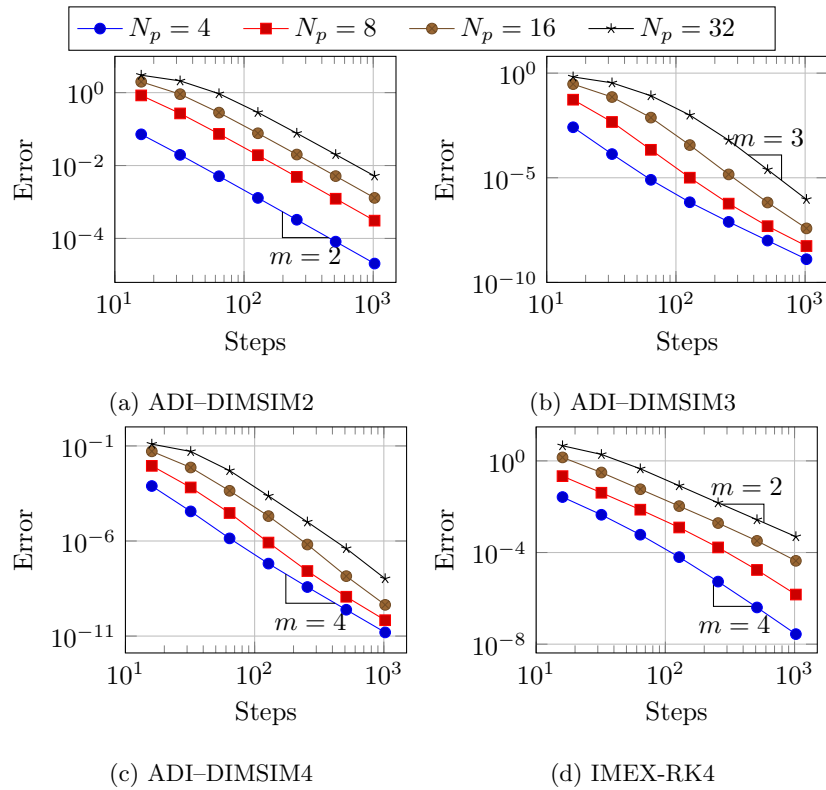


Figure 1: Convergence plots for ADI-DIMSIM methods on 3D test problem compared to IMEX-RK4 method

over the same time-span:

$$\frac{\partial u}{\partial t} = \frac{\partial^2 u}{\partial x^2} + \frac{\partial^2 u}{\partial y^2} + h(x, y, t), \quad (39a)$$

$$h(x, y, t) = e^t(1-x)x(1-y)y + e^t \left(\left(x + \frac{1}{3} \right)^2 + \left(y + \frac{1}{4} \right)^2 - 4 \right) + 2e^t(1-x)x + 2e^t(1-y)y, \quad (39b)$$

with Dirichlet boundary conditions according to the exact solution:

$$u(x, y, t) = e^t(1-x)x(1-y)y + e^t \left(\left(x + \frac{1}{3} \right)^2 + \left(y + \frac{1}{4} \right)^2 \right). \quad (40)$$

Figure 2 shows convergence plots for this experiment. Once again, we observe

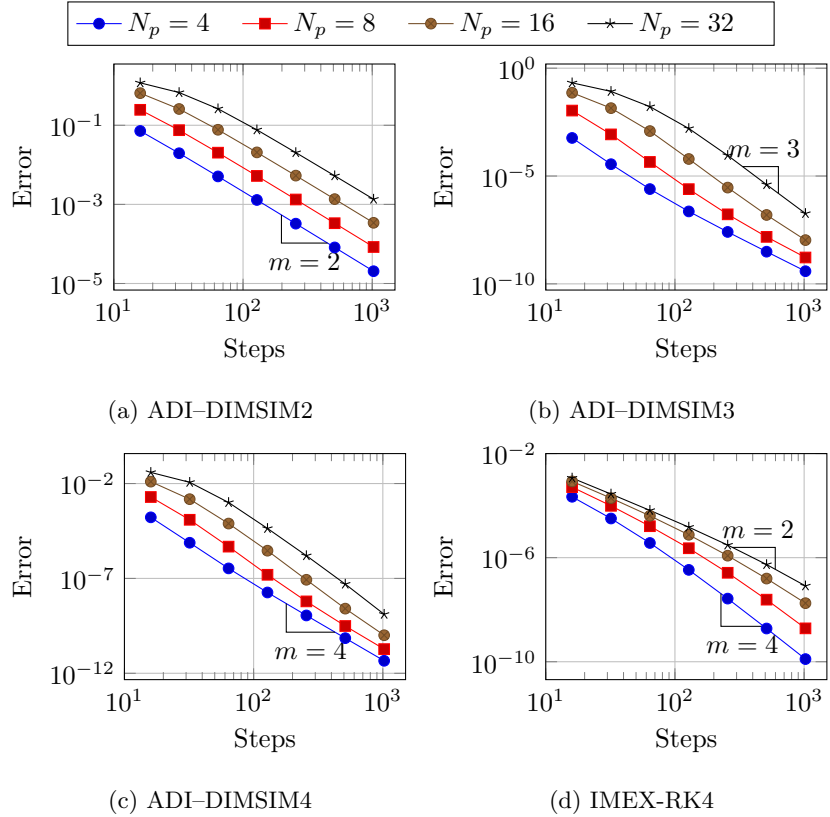


Figure 2: Convergence plots for ADI-DIMSIM methods on 2D test problem compared to IMEX-RK4 method

the order reduction for the IMEX4 Runge-Kutta method in fig. 2d while ADI-DIMSIM methods retain their convergence order in figs. 2a to 2c.

For a third set of experiments, we examine solutions of eq. (39), this time
¹¹⁰ considering the forcing term $g(x, y, t)$ as a third partition to be treated explicitly in the entire integration. This means that the Butcher tableau in eq. (13) is used for these experiments. Figure 3 summarizes the results with close to theoretical order of ADI-DIMSIM methods.

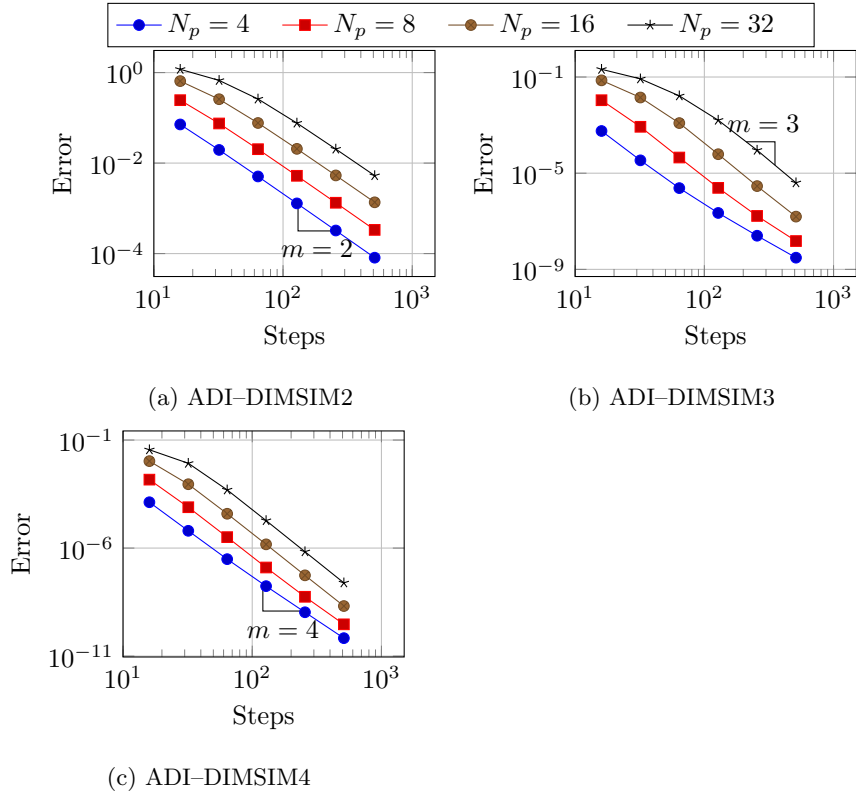


Figure 3: Convergence plots for ADI-DIMSIM methods on 2D test problem with an explicit partition

8. Conclusions

¹¹⁵ This work constructs the new family of GLM-ADI schemes that perform alternating directions implicit integration in the framework of General Linear Methods. Each stage of a GLM-ADI scheme is implicit in a single component of the method, and is explicitly coupled to the other components. This ensures a high computational efficiency. The ADI character of the method stems ¹²⁰ from the fact that consecutive stages are implicit in different partitions, thereby “alternating directions”. Order conditions and stability of these methods are investigated theoretically. The GLM-ADI structure allows for high stage order approximations, and this property alleviates the order reduction observed with other families of schemes.

¹²⁵ Using the new GLM-ADI theory we construct practical ADI-DIMSIM methods of orders two, three, and four. Their design emphasizes stability when applied to parabolic systems where each component has a Jacobian with real negative eigenvalues. Numerical experiments show that the new methods retain their high order of accuracy when applied to parabolic equations with time-¹³⁰ dependent Dirichlet boundary conditions. For these problems where other ADI methods suffer from order reduction.

¹³⁵ The future directions for the authors include extending the current set of methodology to design methods suited for hyperbolic and oscillatory systems and numerical experiments highlighting the computational efficiency of ADI-DIMSIM methods on large scale problems.

Acknowledgments

¹⁴⁰ This work was funded by awards NSF CCF-1613905, NSF ACI-1709727, AFOSR DDDAS FA9550-17-1-0015, and by the Computational Science Laboratory at Virginia Tech. The authors would like to thank Prof. Domingo Hernández Abreu and Mr. Steven Roberts for their valuable comments on this manuscript.

References

References

[1] A. Prothero, A. Robinson, On the stability and accuracy of one-step methods for solving stiff systems of ordinary differential equations, *Mathematics of Computation* 28 (125) (1974) 145–162.

[2] A. Ostermann, M. Roche, Runge–Kutta methods for partial differential equations and fractional orders of convergence, *Mathematics of computation* 59 (200) (1992) 403–420.

[3] Z. Jackiewicz, *General Linear Methods for Ordinary Differential Equations*, Wiley, Hoboken, New Jersey, 2009.

[4] J. Butcher, General linear methods for stiff differential equations, *BIT* 41 (2) (2001) 240–264. doi:10.1023/A:1021986222073.

[5] J. Butcher, W. Wright, The construction of practical general linear methods, *BIT* 43 (4) (2003) 695–721. doi:10.1023/B:BITN.0000009952.71388.23.

[6] H. Zhang, A. Sandu, S. Blaise, Partitioned and implicit-explicit general linear methods for ordinary differential equations, *Journal of Scientific Computing* 61 (1) (2014) 119–144. doi:10.1007/s10915-014-9819-z.

[7] A. Cardone, Z. Jackiewicz, A. Sandu, H. Zhang, Extrapolation-based implicit-explicit general linear methods, *Numerical Algorithms* 65 (3) (2014) 377–399. doi:10.1007/s11075-013-9759-y.

[8] E. Zharovsky, A. Sandu, H. Zhang, A class of IMEX two-step Runge-Kutta methods, *SIAM Journal on Numerical Analysis* 53 (1) (2015) 321–341. doi:10.1137/130937883.

[9] A. Cardone, Z. Jackiewicz, A. Sandu, H. Zhang, Construction of highly-stable implicit-explicit general linear methods, in: M. de Leon, W. Feng,

Z. Feng, J. Gomez, X. Lu, J. Martell, J. Parcet, D. Peralta-Salas, W. Ruan (Eds.), AIMS proceedings, Vol. Dynamical Systems, Differential Equations, and Applications, Madrid, Spain, 2015. doi:10.3934/proc.2015.0185.

[10] H. Zhang, A. Sandu, S. Blaise, High order implicit-explicit general linear methods with optimized stability regions, SIAM Journal on Scientific Computing 38 (3) (2016) A1430–A1453. doi:10.1137/15M1018897.

[11] G. Birkhoff, R. S. Varga, D. Young, Alternating direction implicit methods, in: Advances in computers, Vol. 3, Elsevier, 1962, pp. 189–273.

[12] S. González-Pinto, D. Hernández-Abreu, S. Pérez-Rodríguez, AMF–Runge–Kutta formulas and error estimates for the time integration of advection diffusion reaction PDEs, Journal of Computational and Applied Mathematics 289 (2015) 3–21. doi:10.1016/j.cam.2015.03.048.

[13] S. González-Pinto, D. Hernández-Abreu, S. Pérez-Rodríguez, Rosenbrock-type methods with inexact AMF for the time integration of advection–diffusion–reaction PDEs, Journal of Computational and Applied Mathematics 262 (2014) 304–321. doi:10.1016/j.cam.2013.10.050.

[14] H. Zhang, A. Sandu, P. Tranquilli, Application of approximate matrix factorization to high-order linearly-implicit Runge-Kutta methods, Journal of Computational and Applied Mathematics 286 (2015) 196–210. doi:10.1016/j.cam.2015.03.005.

[15] S. González-Pinto, D. Hernández-Abreu, S. Pérez-Rodríguez, AMF–type W–methods for parabolic problems with mixed derivatives, SIAM Journal on Scientific Computing 40 (5) (2018) A2905–A2929. doi:10.1137/17M1163050.

[16] H. Zhang, A. Sandu, S. Blaise, High order implicit-explicit general linear methods with optimized stability regions, SIAM Journal on Scientific Computing 38 (3) (2016) A1430–A1453.

195 [17] J. Butcher, Z. Jackiewicz, Diagonally implicit general linear methods for ordinary differential equations, BIT 33 (3) (1993) 452–472. doi:10.1007/BF01990528.

[18] Z. Jackiewicz, General linear methods for ordinary differential equations, John Wiley & Sons, 2009.

200 [19] J. Butcher, Z. Jackiewicz, Diagonally implicit general linear methods for ordinary differential equations, BIT Numerical Mathematics 33 (3) (1993) 452–472.

[20] G. Califano, G. Izzo, Z. Jackiewicz, Starting procedures for general linear methods, Applied Numerical Mathematics 120 (2017) 165–175.

205 [21] A. Sandu, M. Günther, A generalized-structure approach to additive Runge-Kutta methods, SIAM Journal on Numerical Analysis 53 (1) (2015) 17–42. doi:10.1137/130943224.

Appendix A. ADI-GLM Methods

Appendix A.1. ADI-DIMSIM2

$$\begin{aligned}
 \mathbf{A}^{\{E\}} &= \begin{pmatrix} 0 & 0 \\ \frac{1}{2} & 0 \end{pmatrix}, \quad \mathbf{W}^{\{E\}} = \begin{pmatrix} 1 & 0 & 0 \\ 1 & \frac{1}{2} & \frac{1}{2} \end{pmatrix}, \quad \mathbf{B}^{\{E\}} = \begin{pmatrix} \frac{1}{2} & -\frac{5}{32} \\ 0 & \frac{27}{32} \end{pmatrix}, \\
 \mathbf{W}^{\{I\}} &= \begin{pmatrix} 1 & -\frac{5}{8} & 0 \\ 1 & \frac{1}{8} & -\frac{1}{8} \end{pmatrix} \quad \mathbf{A}^{\{I\}} = \begin{pmatrix} \frac{5}{8} & 0 \\ \frac{1}{4} & \frac{5}{8} \end{pmatrix}, \quad \mathbf{B}^{\{I\}} = \begin{pmatrix} -\frac{3}{128} & \frac{5}{128} \\ \frac{13}{128} & \frac{85}{128} \end{pmatrix}, \\
 v &= \left(-\frac{5}{16} \quad \frac{21}{16} \right)^T, \quad \mathbf{c} = \left(0 \quad 1 \right)^T.
 \end{aligned}$$

$$\begin{aligned}
 \mathbf{A}^{\{E\}} &= \begin{pmatrix} 0 & 0 & 0 \\ \frac{1}{3} & 0 & 0 \\ \frac{1}{3} & \frac{1}{3} & 0 \end{pmatrix}, \quad \mathbf{W}^{\{E\}} = \begin{pmatrix} 1 & 0 & 0 & 0 \\ 1 & \frac{1}{6} & \frac{1}{8} & \frac{1}{48} \\ 1 & \frac{1}{3} & \frac{1}{3} & \frac{1}{8} \end{pmatrix}, \\
 \mathbf{B}^{\{E\}} &= \begin{pmatrix} \frac{1282023}{4000000} & \frac{346069}{1500000} & \frac{1077517}{4000000} \\ \frac{6346069}{12000000} & -\frac{217977}{500000} & \frac{3577517}{4000000} \\ \frac{13846069}{12000000} & -\frac{3153931}{1500000} & \frac{25232551}{12000000} \end{pmatrix}, \\
 \mathbf{A}^{\{I\}} &= \begin{pmatrix} \frac{1}{3} & 0 & 0 \\ \frac{128195845}{365740056} & \frac{1}{3} & 0 \\ -\frac{2102253}{6772964} & \frac{2}{3} & \frac{1}{3} \end{pmatrix}, \\
 \mathbf{W}^{\{I\}} &= \begin{pmatrix} 1 & -\frac{1}{3} & 0 & 0 \\ 1 & -\frac{67239169}{365740056} & -\frac{1}{24} & -\frac{1}{48} \\ 1 & \frac{2102253}{6772964} & -\frac{1}{6} & -\frac{1}{12} \end{pmatrix}, \\
 v &= \left(-\frac{153931}{500000} \quad \frac{153931}{100000} \quad -\frac{28931}{125000} \right)^T, \quad \mathbf{c} = \left(0 \quad \frac{1}{2} \quad 1 \right)^T.
 \end{aligned}$$

$$\begin{aligned}
\mathbf{A}^{\{E\}} &= \begin{pmatrix} 0 & 0 & 0 & 0 \\ \frac{1}{2} & 0 & 0 & 0 \\ 0 & \frac{1}{2} & 0 & 0 \\ 0 & 0 & 1 & 0 \end{pmatrix}, \quad \mathbf{W}^{\{E\}} = \begin{pmatrix} 1 & 0 & 0 & 0 \\ 1 & -\frac{1}{6} & \frac{1}{18} & \frac{1}{162} \\ 1 & \frac{1}{6} & \frac{1}{18} & \frac{7}{324} \\ 1 & 0 & -\frac{1}{6} & -\frac{1}{18} \end{pmatrix}^T, \\
\mathbf{B}^{\{E\}} &= \begin{pmatrix} -16614547665931691 & 4381680037003501 & 20674462877195909 & -166249057 \\ -22416811736319120 & 67250435208957360 & 13450087041791472 & -1646244720 \\ -19416649132971581 & 12980310487942937 & 321762125778353225 & 89392211 \\ -22416811736319120 & 22416811736319120 & 4483362347263824 & 548748240 \\ -75996590023500713 & 101521197561053021 & -4731257090632427 & 1479995663 \\ -67250435208957360 & 67250435208957360 & 13450087041791472 & 1646244720 \\ \frac{3000162603347539}{22416811736319120} & -\frac{22258853879327589}{67250435208957360} & \frac{8288115445481467}{13450087041791472} & -\frac{3664519087}{1646244720} \end{pmatrix}, \\
\mathbf{A}^{\{I\}} &= \begin{pmatrix} 1 & 0 & 0 & 0 \\ \frac{62202553}{133059146} & 1 & 0 & 0 \\ -\frac{45821383}{145345738} & -\frac{21680437}{51644911} & 1 & 0 \\ -\frac{85837310}{42991027} & -\frac{176998631}{169118203} & \frac{4352681}{84793584} & 1 \end{pmatrix}, \\
\mathbf{W}^{\{I\}} &= \begin{pmatrix} 1 & -1 & 0 & 0 & 0 & 0 \\ 1 & -\frac{452725951}{399177438} & -\frac{5}{18} & -\frac{4}{81} & -\frac{11}{1944} \\ 1 & \frac{311945978804791}{776520796886826} & -\frac{141538333}{464804199} & -\frac{1250933575}{8366475582} & -\frac{967856909}{25099426746} \\ 1 & \frac{1844967356089388680167}{616497283673183554289904} & -\frac{3987047360167655}{21510207828014328} & -\frac{18494238345570695}{64530623484042984} & -\frac{70317099526056967}{580775611356386856} \end{pmatrix}, \\
v &= \begin{pmatrix} \frac{475732812567067}{467016911173315} & -\frac{39531533}{22864510} & -\frac{23670237}{81701626} & 2 \end{pmatrix}^T, \quad \mathbf{c} = \begin{pmatrix} 0 & \frac{1}{3} & \frac{2}{3} & 1 \end{pmatrix}^T.
\end{aligned}$$

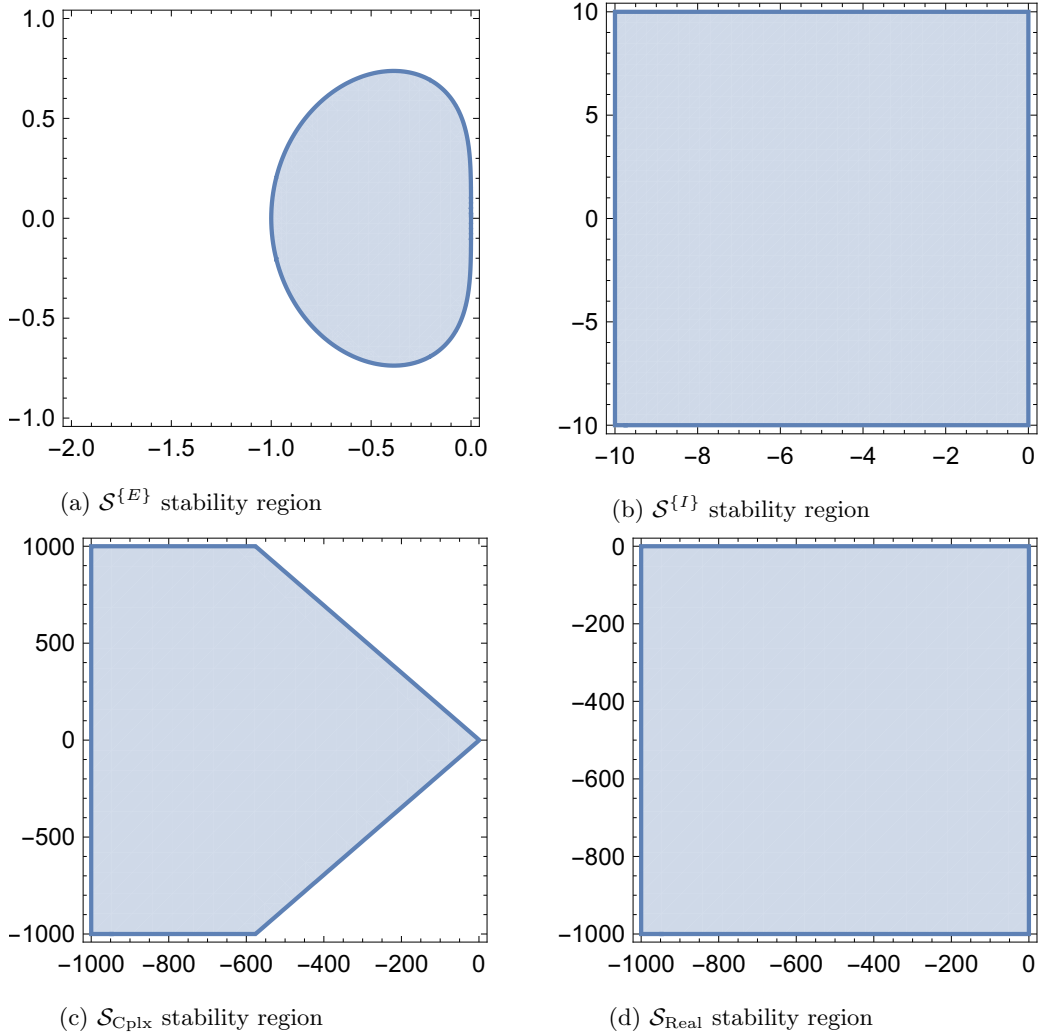


Figure B.4: Stability plots for ADI–DIMSIM2 method

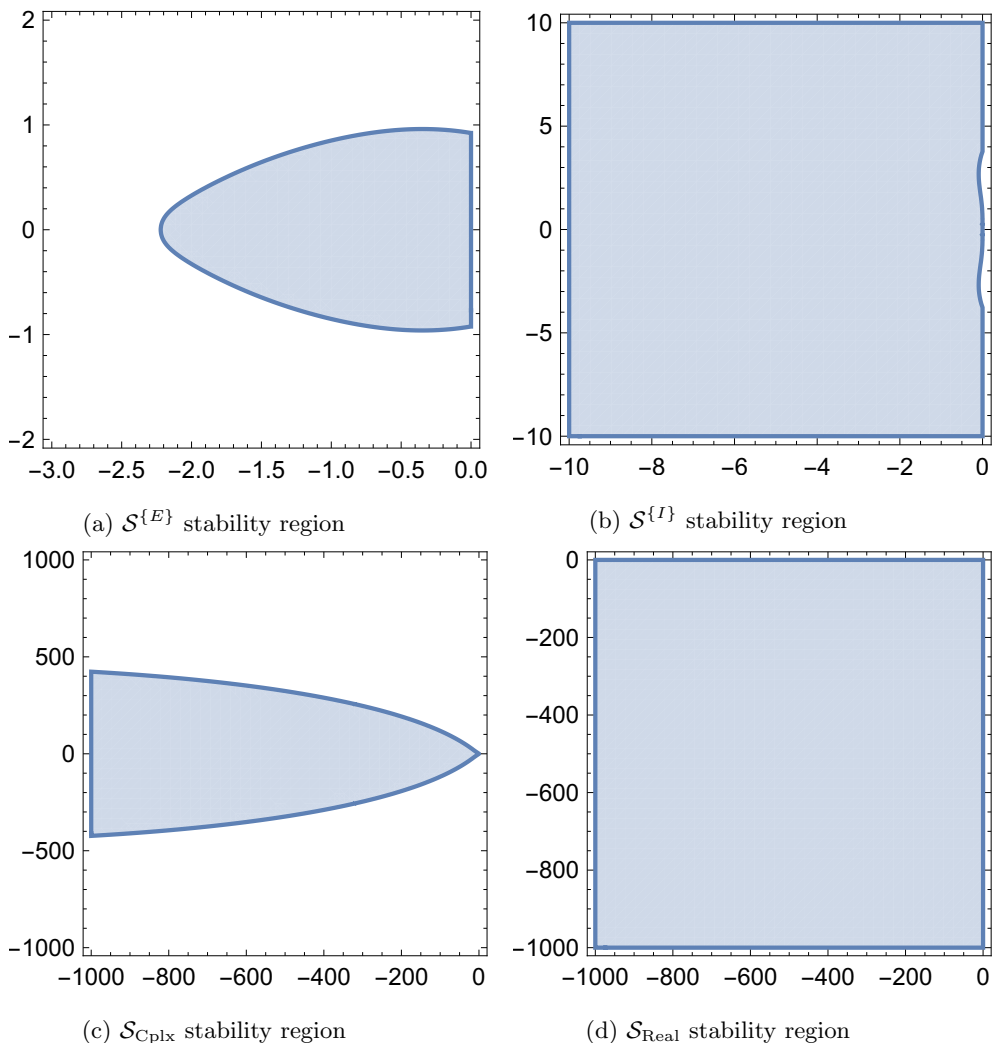


Figure B.5: Stability plots for ADI-DIMSIM3 method

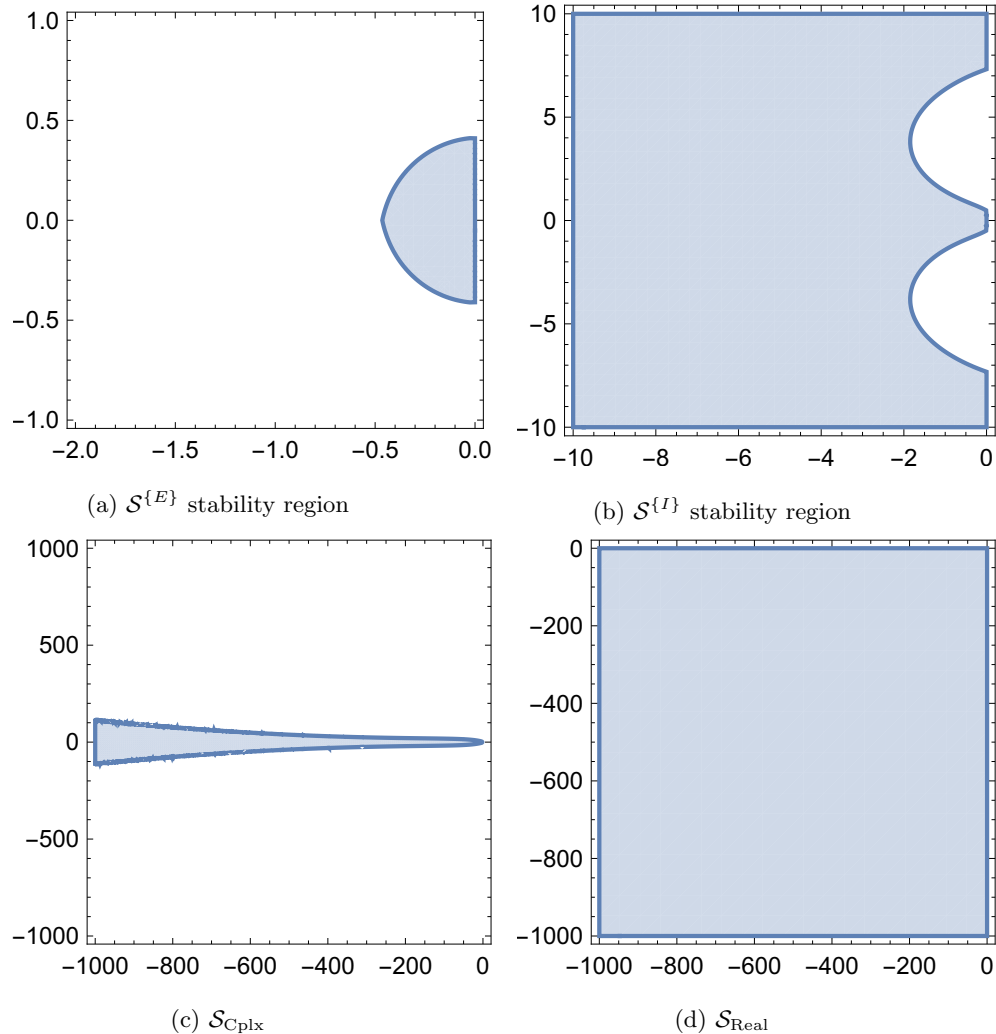


Figure B.6: Stability plots for ADI–DIMSIM4 method